Preparation and soft lithographic printing of nano-sized ITO-dispersions for the manufacture of electrodes for TFTs

Nadja Straue · Martin Rauscher · Sabine Walther · Hendrik Faber · Andreas Roosen

Abstract The production of printed electronics exhibits an enormous economical potential due to the possibility to manufacture innovative products at low cost. At the moment, one of the major challenges for the fabrication of printed electronics is the controllability of the material properties during processing and the miniaturization of the deposited structures. In this context, the application of soft lithographic techniques appears promising, because they allow a defined patterning of the materials in the range of few nanometers, which is far below the limits of other printing techniques like inkjet-printing or screen printing. This work proves the applicability of the soft lithographic technique micro-molding in capillaries (MIMIC) for the manufacture of conductive indium tin oxide (ITO) electrodes. For the creation of stable dispersions of ITO nano-sized particles, steric as well as electrostatic stabilization concepts are applied. The prepared dispersions are characterized with regard to the later processing via MIMIC. The geometry and the electrical properties of the soft lithographically deposited structures are determined to prove their functionality. Special attention is paid to the influence of the wetting behavior of the dispersions on the resulting geometry of the structures. Finally, the applicability of the optimized structures is demonstrated by the assembly of a thin film transistor (TFT), in which the deposited structures serve as source and drain electrodes.

Introduction

The fabrication of printed electronics is gaining increasing interest due to the broad range of future applications. Complex devices like flexible displays, solar cells, and sensors as well as simple circuits for disposable electronics, like RFID tags for labeling can be manufactured [1–3]. For this technology, which is in the stage to enter the market, the printing of nano-sized particle dispersions appears promising. Such inks are suitable to be processed via classical printing technologies. Furthermore, nano-particles exhibit the tendency to sinter at very low temperatures due to their high surface to volume ratio. Thus, the manufacture of functional layers and structures on flexible polymer substrates is enabled.

In this work, the applicability of the soft lithographic technique micro-molding in capillaries (MIMIC) for the manufacture of conductive functional structures made from dispersions of nano-sized particles is investigated. Soft lithography represents a versatile non-photolithographic method for micro- and nano-fabrication, which can be applied to a wide range of potential applications in surface chemistry, materials science [4], optics, MEMS [5], and microelectronics [6–10]. The common feature of soft lithographic techniques is the use of an elastomeric stamp with a structured surface to pattern structures with feature sizes ranging from 30 nm to 100 μm [11].

N. Straue (✉) · M. Rauscher · A. Roosen
Department of Materials Science, Glass and Ceramics, University of Erlangen-Nuremberg, Martensstrasse 5, 91058 Erlangen, Germany
e-mail: nadja.straue@ww.uni-erlangen.de
URL: http://www.glass-ceramics.uni-erlangen.de/

S. Walther
Department of Electrical, Electronic and Communication Engineering, Electron Devices, University of Erlangen-Nuremberg, Cauerstrasse 6, 91058 Erlangen, Germany

H. Faber
Department of Materials Science, Polymer Materials, University of Erlangen-Nuremberg, Martensstrasse 5, 91058 Erlangen, Germany

High standards are set on the quality of the inks, dispersions, and solutions to create patterns in these dimensions. If dispersions containing particles are used, they need to be very well dispersed to guarantee a print result of high quality. Stabilization of particles thus plays a key role in nano- and microfabrication [12–16]. Aside from intensive research, efforts for the commercialization of soft lithographic techniques in the field of large-area electronics are taking place. The main challenge for the industrialization includes the development of reliable techniques to achieve registration of the printed patterns to existing features on a substrate [17].

Especially, the MIMC process features an extremely high resolution and is superior to the other soft lithographic techniques because it allows to create structures without a particulate background beyond the confinements of the pattern on the substrates. The principle processing steps of MIMIC are shown in Fig. 1. The patterned stamp, which exhibits open channels, is pressed onto a substrate and a drop of a dispersion or solution is placed at the open end of the channel and infiltrates the channel due to capillary forces. When the solvent evaporates, the residual material dries within the confinement of the mold.

In this work, soft lithographic structures are deposited and characterized to investigate their applicability as conductive paths in field effect transistors. A nano-sized indium tin oxide (ITO) powder is applied as a model material. Due to the potential of the ITO powder to form coatings and structures with a high optical transmission and a low electrical resistance, printed ITO structures could be applied in devices requiring transparent, conductive structures, e.g., in electron devices for flexible displays, flexible solar cells, etc.

Experimental procedure

Preparation of dispersions

For the development of stable dispersions, a nano-sized ITO powder (VP Adnano® ITO TC 8, Evonik Degussa GmbH, Marl, Germany) with a primary particle size in the range of 10 to 20 nm and an agglomerate size above
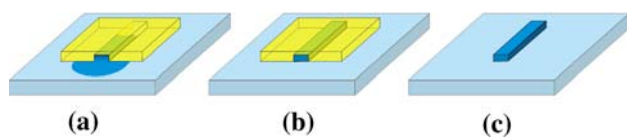

Fig. 1 Schematic illustration of the MIMIC process: **a** a drop of dispersion is placed on the substrate at the opening of a channel in the stamp; **b** the dispersion infiltrates the structure due to capillary forces and dries within the confinement of the mold; **c** the structure replicates the stamp geometry

100 nm was applied. The specific surface area of the powder was determined by BET measurements to be 47.6 m^2/g (ASAP 2000, Micromeritics Instrument Corp., Norcross/GA, USA). Two stabilization concepts were realized: for the sterically stabilized ethanol-based dispersion, the carbon acid 2-[2-(2-methoxy)ethoxy]acetic acid (Sigma Aldrich, Milwaukee, WI, USA), also called 3,6,9-trioxadecanoic acid or TODS, was used as dispersing agent. For the electrostatically stabilized water-based dispersion, the salt $InCl_3$ (Merck KGaA, Darmstadt, Germany) was used.

Sterically stabilized ethanol-based dispersions with varied ITO concentrations in the range of 5 to 60 wt% (0.58–14.41 vol.%) and 3 wt.% (0.18 vol.%) TODS with respect to the solids content were prepared in PE bottles with ZrO_2 milling balls ($d_{50} \sim 3.5$ mm), which were agitated in a tumbling mixer (Turbula, Willy A. Bachofen AG, Basel, Swiss) for at least 24 h. The optimum dispersant content of the long-term stable sterically stabilized dispersions had been determined to be 3 wt% (0.18 vol.%) with respect to the solids content in preliminary rheological and adsorption isotherm experiments.

From the dispersion with 35.5 wt% (5.77 vol.%) particle content, a milled dispersion with a smaller aggregate size was produced by milling in a stirred media mill (Type 4V1 M, Netzsch GmbH, Selb, Germany) at 950 rpm for 2 h, using ZrO_2 milling balls ($d_{50} \sim 100$ μm). Subsequently, ethanol was used to rinse the dispersion off from the milling balls, which lead to a thinning of the dispersion down to 18.6 wt% (2.47 vol.%) solids content.

Electrostatically stabilized dispersions with varied solids contents in the range of 10 to 35.5 wt% (1.53–7.16 vol.%) were produced by adding 10^{-4} mol/L $InCl_3$ and the nanopowder to deionized water. The optimum salt content of the electrostatically stabilized dispersions had been determined by means of zeta potential measurements (Nano ZEN 3600, Malvern Instruments Ltd, Worcestershire, UK), DLVO calculations and sedimentation tests preliminarily. The electrostatically stabilized dispersions were processed in PE bottles with ZrO_2 milling balls ($d_{50} \sim 3.5$ mm) in the tumbling mixer for at least 24 h.

Characterization of dispersions

The viscosity of the ethanol-based and water-based dispersions with different solids contents was analyzed by means of a rheometer (Physica UDS 200, Paar Physica, Stuttgart, Germany). A cone/plate arrangement was used with a cone diameter d_{cone} of 25 mm and an angle of 2° at a temperature of 20 °C. A shear rate of 200 s^{-1} was applied for 60 s. The chosen shear rate is in the same order of magnitude as the shear rates, which occur during the infiltration of the stamps in the MIMIC experiments.

Additionally, the particle size of the ITO in the long-term stable ethanol-based dispersions with different solids contents was analyzed with dynamic light scattering experiments (Ultra Fine Particle Analyzer UPA150, Microtrac, North Lago, USA). Before the measurement, the dispersions were homogenized with an ultrasonic finger for 1 min (Ultraschallprozessor UP 2005, Hielscher Ultrasonics GmbH, Teltow, Germany).

MIMIC experiments

To fabricate stamps for the MIMIC infiltration experiments, the pattern of a photolithographically structured silicon master was transferred to polydimethylsiloxane (PDMS) stamps (Sylgard 184, Dow Corning, USA), which were processed according to standard procedures. An oligomere mixture of the main component and the cross linking agent of the PDMS was prepared in the ratio 10:1. This mixture was subsequently poured over the master, which was coated with an antisticking layer [18], and cured for at least 30 h at room temperature. Elevated temperatures in a furnace were not applied to allow the buoyancy of air bubbles. Two different types of stamps were used in this work: Type I featured a linear channel with rectangular cross section and served as model structure for investigations. The angled structure of Type II exhibited also a rectangular cross section. Type II was used to print source-drain-electrodes for the construction of a thin film transistor (TFT). Both structures had a channel height of 2.5 µm. A schematic top view of the stamps can be seen in Fig. 2.

Stamps with untreated and functionalized surfaces, respectively, were used to study the influence of the contact angle between ink and stamp on the resulting geometry of the structure. A hydrophilic surface was created by surface

Fig. 2 Schematic top view of the used stamps; **a** stamp of Type I, **b** stamp of Type II

oxidation of the stamps via plasma treatment for 240 s at 250 W (PlasmaClean 4, Ilmvac, Ilmenau, Germany). As this oxidation is not long-term stable, a quick further processing was always assured [19]. A hydrophobic surface was generated by attaching 1H,1H,2H,2H-perfluorodecyltrichlorsilane (PFDTS) molecules to the surface by molecular vapor deposition (MVD 100, Applied Microstructures, San Jose, CA, USA). First, an oxygen plasma treatment was applied to the PDMS stamp for 300 s at 150 W, before the PFDTS was deposited for 900 s. All stamps were rinsed with isopropanol to remove dust before they were used.

For the prints different substrates were used: structures of Type I were printed on LCD glass AF 37 (Schott Display GmbH, Jena, Germany). Structures of Type II, which were used for the assembly of a TFT, were deposited on a thermally oxidized silicon wafer with an oxide layer thickness of 200 nm (Chair of Electron Devices, University of Erlangen-Nuremberg, Germany). Substrates were also cleaned with isopropanol before further processing.

Previous to the infiltration, the dispersions used were homogenized by a treatment with the ultrasonic finger for 1 min. To infiltrate the stamps, they were evenly pressed onto the substrates and a drop of dispersion was applied at one of the open ends of the channel. The drop spontaneously infiltrated the stamp during few seconds due to capillary forces. The drying was conducted in ambient conditions for few minutes before the stamp was lifted off. Selected structures were thermally treated in air to improve their electrical conductivity [20]. The heating and the cooling rate were 5 °C/min and the holding time at the peak temperature of 500 °C was 30 min.

Contact angle measurements were conducted to analyze the wetting behavior of the dispersions on various substrate and stamp materials (Contact Angle System OCA 30, Dataphysics Instruments, Filderstadt, Germany).

Characterization of printed structures

The geometry as well as the electrical properties of the produced structures were analyzed. Topographical pictures of the structures were taken with a confocal microscope (µsurf custom microscope, Nanofocus, Oberhausen, Germany). Micrographs of structures of Type I were taken from areas opposite to the opening, where the infiltration was conducted, because the structures were most homogenous at this position. The arithmetic average roughness R_a of the structures was calculated over a length of 25 µm by using the data of the topographical pictures. In case of high waviness of the specimens, extreme corrugations were subtracted by the computer software before the surface roughness was calculated. All measured parameters were averaged over at least three samples. Furthermore, measurements of the current–voltage characteristics of printed
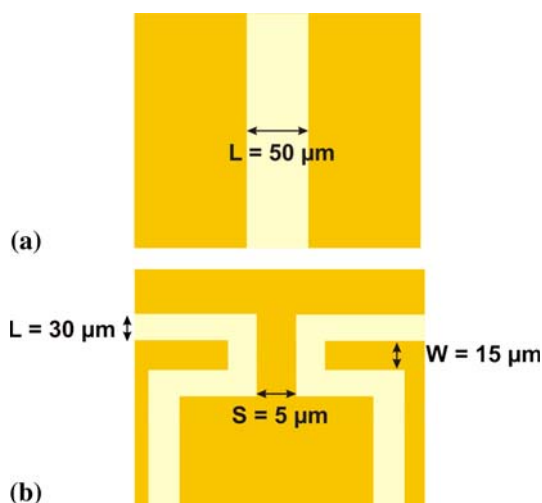
structures of Type I were conducted (Parameter Analyzer Type HP4156a, Hewlett-Packard, Palo Alto, USA).

TFT assembly

In order to demonstrate the functionality of the printed structures, a bottom gate assembled TFT was realized. Structures of Type II were printed using the ethanol-based sterically stabilized dispersion with 20 wt% (2.70 vol.%) ITO. A thermally oxidized wafer was used as the bottom gate electrode and the gate dielectric. In order to increase the electrical conductivity of the structures, the prints were thermally treated up to 500 °C. A semiconducting layer between the soft lithographically deposited ITO source and drain electrodes was deposited by spin coating a sterically stabilized dispersion with 20 wt% (3.47 vol.%) zinc oxide (VP Adnano® ZnO 20, Evonik Degussa GmbH, Marl, Germany) in ethanol at a rotational speed of 2,500 rpm and a spin coating time of 30 s. To evaporate the residual solvent, the device was placed on a hot plate at 120 °C for 30 s. Subsequently, a final tempering step was carried out at 300 °C for 30 min. A schematic drawing of the TFT is shown in Fig. 3.

The electrical characteristics of the TFT were recorded under N_2-atmosphere because the conductivity of ZnO is very sensitive to humidity (Parameter Analyzer Type HP4145, Hewlett-Packard, Palo Alto, USA). Additionally, the measurements were carried out in a dark chamber to avoid light-initiated processes in the semiconducting ZnO.

Results and discussion

Properties of the dispersions

The apparent viscosity at a shear rate of 200 s^{-1} in dependence on the solids content for the electrostatically stabilized water-based dispersions and the sterically stabilized ethanol-based dispersions is depicted in Fig. 4. All analyzed viscosities are in the range of 1 to 100 mPas and are thus low enough to infiltrate the microchannels during the MIMIC process. As expected, the viscosity of the dispersions rises with increasing solids content. Additionally, it can be seen that the viscosities of the ethanol-based dispersions are generally lower than the viscosities of the
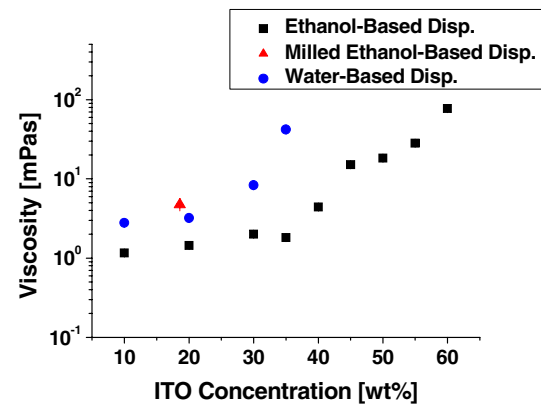

Fig. 4 Viscosity of ethanol-based and water-based dispersions at 200 s^{-1} in dependence on the solids content; the ethanol-based dispersion with 18.6 wt% ITO was additionally milled

water-based dispersions at same solids content. Furthermore, the water-based dispersions exhibit a steeper rise in viscosity with increasing particle content. These facts and the observation that the water-based dispersions are only short-term stable lead to the conclusion that strong attractive interactions exist between the ITO particles in the water-based electrostatically stabilized dispersions. However, the low viscosity of the ethanol-based dispersions over a broad ITO concentration range of 10 to 35.5 wt% (1.22–5.77 vol.%) and the observation that particles in these dispersions did not sediment over months, indicate that the stabilization with the carbon acid TODS is very effective. Milling of the ethanol-based dispersion with 18.6 wt% (2.47 vol.%) ITO resulted in an increase in viscosity. This could be due to an increase in specific surface area relative to the volume by the milling effect or by the degradation of the dispersant used.

The analysis of the particle size in the long-term stable ethanol-based sterically stabilized dispersions in dependence on the solids content shown in Fig. 5 confirms that the stabilization in the ITO concentration range between 10 and 35.5 wt% (1.22–5.77 vol.%) is very effective because the $d_{vol,50}$ of ITO in these dispersions varies between 93 and 102 nm and no significant increase in the aggregate size can be observed for increasing solids contents. At higher solids concentrations in the range of 40 to 60 wt% (6.91–14.41 vol.%), a significant increase in agglomerate size $d_{vol,50}$ up to ~130 nm can be observed. Due to the higher tendency of agglomeration in the dispersions at higher solids contents, the ITO concentration was generally limited to 35.5 wt% (5.77 vol.%) in the following experiments. Furthermore, the dynamic light scattering experiment proved the success of the milling procedure. The diameter $d_{vol,50}$ of the ITO aggregates could be significantly reduced to 35.2 nm in the dispersion, which was treated in the stirred media mill.
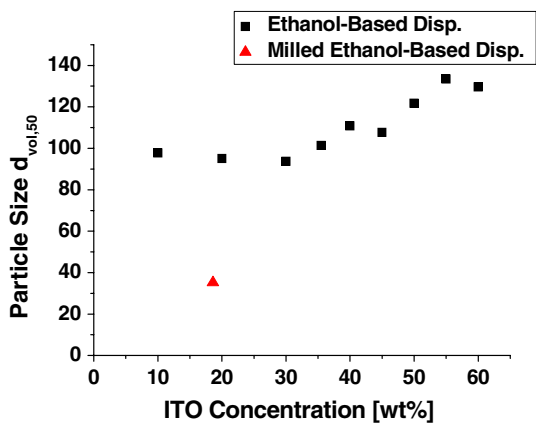

Fig. 3 Schematic of the TFT assembly used in this work

Fig. 5 Particle size $d_{vol.50}$ of particles in the ethanol-based dispersions; the dispersion with 18.6 wt% (2.47 vol.%) ITO was additionally milled

Geometrical and electrical properties of the deposited structures

First MIMIC infiltration experiments showed the superior quality of the ethanol-based dispersions and their suitability for the processing via soft lithographic methods. Figure 6 depicts the topographical pictures of two structures of Type I printed on LCD glass with the ethanol-based and the water-based dispersions, which both contained 20 wt% ITO, i.e., 2.70 vol.% in the sterically stabilized dispersion and 3.38 vol.% in the electrostatically stabilized dispersion. The structure, which was produced using the water-based dispersion, exhibits island-like aggregates on a merely covered substrate. Obviously, the structure printed with the ethanol-based dispersion is more homogeneous and shows a good reproduction of the stamp geometry. However, as indicated in the picture by the bright stripe in the middle and the dark stripe at the edges, the structure features no rectangular cross section. A double-peak shape of the deposited structure can be observed: The height in the middle is smaller than at the edges.
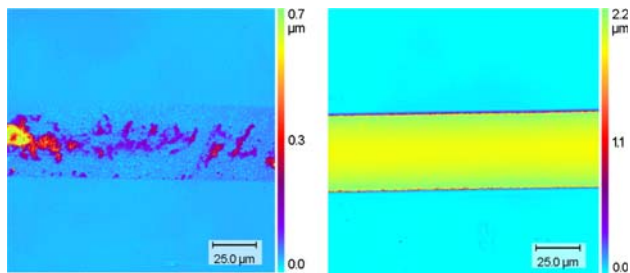
Table 1 Contact angles between water-based and ethanol-based dispersions with 20 wt% ITO, i.e., 2.70 vol.% ITO in the ethanol-based dispersion and 3.38 vol.% in the water-based dispersion, and the materials used as substrates and stamps

Material	Ethanol-based dispersion (°)	Water-based dispersion (°)
LCD glass	14.47	48.7
Untreated stamp	41.1	105.9

The differences between the structures printed with the two different dispersions can be explained by the wetting behavior of the dispersions. Due to the higher surface tension of water (72.8 mN/m) compared to ethanol (22.3 mN/m [21]), the contact angle of the water-based dispersion on the substrate as well as on the used stamp is much higher than the contact angle between the ethanol-based dispersion on the substrate or the stamp, respectively (Table 1). This insufficient wetting behavior of the water-based dispersions results in an insufficient print result. In further work, the wetting behavior of water-based systems could be adapted by the addition of surfactants, but a negative effect due to the addition of processing additives on the electrical properties of the deposited structures needs to be expected. For this reason, only ethanol-based inks were used to further study the influences of various parameters on the deposited structures.

For further characterization of the geometry of the printed structures of Type I, the parameters arithmetic average roughness R_a of the deposited structures and the relative height difference between the edges of the structures and the middle, also called height depression in this work, was measured. In general, a low roughness and a good reproduction of the stamp geometry, i.e., a low height depression, was desired. Results are depicted in Fig. 7. The
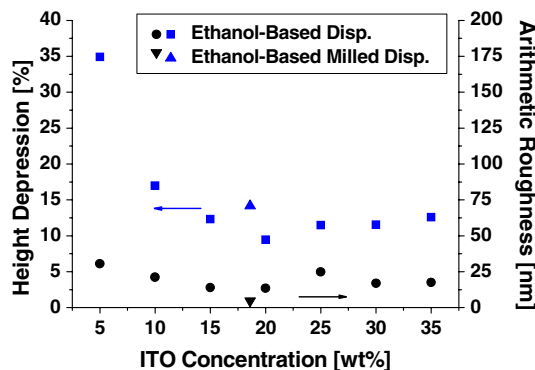

Fig. 6 Topographical picture of structures of Type I on LCD glass printed with untreated stamps; *left*: structure printed with water-based dispersion of 20 wt% (2.70 wt%) ITO, *right*: structure printed with ethanol-based dispersion of 20 wt% (3.38 vol.%) ITO

Fig. 7 Dependence of the geometrical parameters height depression and arithmetic roughness of structures of Type I on ITO concentration. Structures were printed with ethanol-based dispersions and untreated stamps on LCD glass; the ethanol-based dispersion with 18.6 wt% ITO was additionally milled

height at the edges of the depicted structures is in the range of 1.7 to 2.2 μm.

The measured values of height depression are in the range of 10 to 65% and the values for the arithmetic roughness are in the range of 5 to 30 nm. The height depression drops with increasing solids content. Printed structures made of dispersions with low solids content in the range of 5 to 15 wt% (0.58–1.92 vol.%) do not contain enough particles to fill the channel after drying. This leads to a large height depression and comparably high roughness. Above a concentration of 20 wt% (2.70 vol.%) ITO in the dispersion, no further reduction of the height depression or the roughness can be observed. Due to the increased tendency of the ethanol-based dispersions to agglomerate at high solids contents, an optimum solids content of 20 wt% (2.70 vol.%) ITO was determined for successive MIMIC experiments. Besides the concentration, also a significant influence of the agglomerate size in the dispersion on the shown parameters is visible; the reduced agglomerate size in the milled dispersion results in a lower roughness. Furthermore, the smaller degree of agglomeration favors a higher density of the printed structures and thus a higher height depression.

Experiments that aimed to deposit an insulating polymer layer onto the printed structure via spin coating failed and therefore further work focused on the adaptation of the geometry of the structures.

In order to further optimize the geometry of the deposited structures, the surface of the stamps, which were used to soft lithographically deposit the structures, was functionalized as described above. Thus, additionally to the untreated stamps, plasma-treated hydrophilic and PFDTS-functionalized hydrophobic stamps were created. The success of this functionalization was assured by contact angle measurements (Table 2).

The results of the contact angle measurements further show, too, that the agglomerate size also influences the wetting behavior. A smaller agglomerate size generally favors a higher contact angle between dispersion and stamp. It was proven by a reference measurement with a non-milled sterically stabilized dispersion with a solids content of 15 wt% (1.92 vol.%) that this effect is not caused by the solids content in the dispersion, as the analyzed non-milled dispersions with 15 wt% (1.92 vol.%) ITO and 20 wt% (2.70 vol.%) ITO exhibited the same contact angles on the stamps. The contact angle of the sterically stabilized dispersion with 15 wt% (1.92 vol.%) ITO on the untreated PDMS, e.g., was determined to be 41.3°.

Topographical pictures, related height profiles and measured geometrical parameters are presented in Table 3. Due to their lower height depression compared to structures printed with the milled dispersion, structures deposited with an ethanol-based non-milled dispersion and 20 wt% (2.70 vol.%) ITO are presented. It is clearly visible that all deposited structures shown do not exhibit a rectangular, but a double peak-shaped cross section. This can be assigned to the drying process. Due to the higher localized pressure in zones with small radii of curvature, the dispersion preferentially wets the corners of the stamp. During drying, the structure debonds first from the flat PDMS walls and remains pinned in the corners, which leads to the double-peak topography [22]. The sagging of the stamp, which is a known problem of the MIMIC process [23–25], can be assumed to have a negligible influence on the double-peak topography in this work. This is confirmed by the geometrical data of the print, which was deposited by using the hydrophobic stamp. The deposited structure features a height at the edges of only about 60% of the stamp height but exhibits the height depression nevertheless. In case of the use of the hydrophobic stamp, the dispersion appears to be pinned to the PDMS walls during drying.

The structure printed with the hydrophobic stamp exhibits a much smaller height than the other shown structures. Due to the high contact angle between the dispersion and the hydrophobic stamp, only a small amount of dispersion infiltrates the stamp. In contrast, the low wetting angle between the dispersion and the hydrophilic stamp results in a higher height at the edges compared to the structure printed with the untreated stamp. Due to high adhesion forces between dispersion and stamp very steep flank angles of the print deposited with the hydrophilic stamp can be observed. This effect results also in an increased height depression of this structure compared to the structure printed with the untreated stamp. The highest relative height depression can be observed for the structure deposited with the hydrophobic stamp, as nearly no particles are deposited in the middle of the structure.
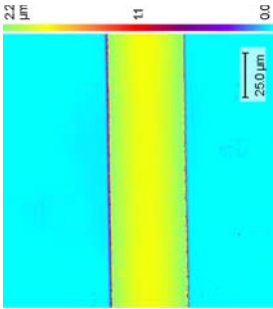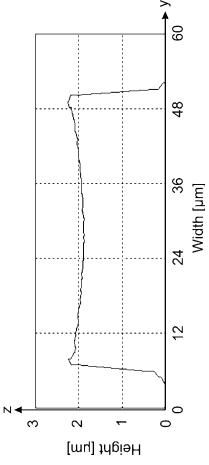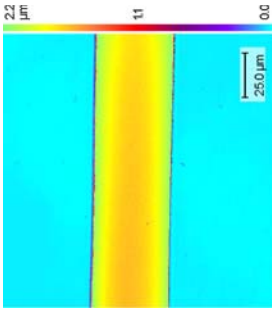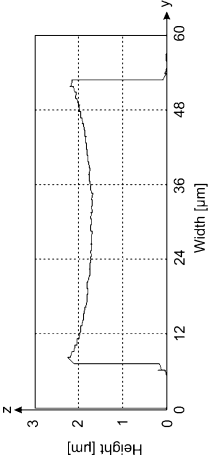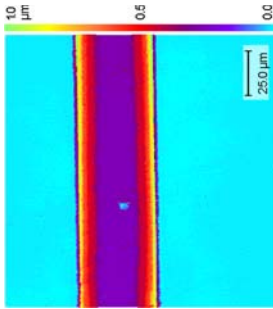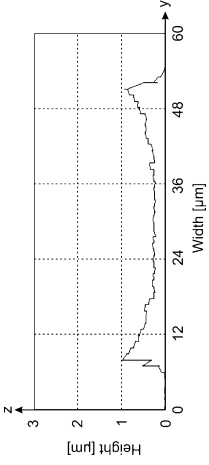
Besides the height of the structures, the surface-functionalization has a significant impact on the roughness of the deposited structures, too. Lowest roughness is observed for prints with hydrophilic stamps, whereas structures deposited with hydrophobic stamps exhibit highest roughness. In the latter case, the non-uniform drop formation due

Table 2 Contact angles between ethanol-based dispersions and untreated and functionalized stamps

Material	Ethanol-based dispersion, c(ITO) = 20 wt% (2.70 vol.%) (°)	Ethanol-based milled dispersion, c(ITO) = 18.6 wt% (2.47 vol.%) (°)
Untreated stamp	41.1	49.6
Hydrophilic stamp	∼3[a]	25.7
Hydrophobic stamp	55.8	61.6

[a] The contact angle could not be determined exactly, as instantaneous spreading of the dispersion took place

Table 3 Overview of properties of structures of Type I printed with the 20 wt% (2.70 vol.%) ITO ethanol-based dispersion on LCD glass

Stamp	Topographical picture	Height profile	Height at the edges (µm)	Height depression (%)	Roughness R_a (nm)
Untreated stamp			2.12	9.43	13.53
Hydrophilic stamp			2.23	18.83	8.53
Hydrophobic stamp			1.06	64.26	14.47

to the high contact angle causes high roughness of the print. In contrast, the stronger adhesion of the dispersion to the hydrophilic PDMS stamp during drying leads to a better reproduction of the flat walls of the stamp.

In conclusion, surface-functionalization is an adequate tool to adapt the shape of the deposited structure without changing the geometry of the stamp. The best reproduction of the stamp geometry is observed for non-functionalized stamps. If a very low roughness of the structures is required, hydrophilic plasma-treated stamps should be used. To achieve a reduced height of the deposited structures, hydrophobic FDTS-functionalized stamps should be applied.

The measurements of the electrical conductivity of the deposited structures of Type I showed that it is not influenced by the surface functionalization. In a thermally untreated state, the specific electrical resistance of the structures was about 137 Ω cm. The specific electrical resistance could be lowered to 0.51 Ω cm by a thermal treatment at 500 °C due to the formation of sinter necks. These values are clearly above the resistances that can be reached with sputtered layers due to the minor morphological quality of the particulate structures [20, 26]. However, the conductivity is sufficient to supply the electrode function in a printed TFT.

Characteristics of the TFT

In order to prove the applicability of the printed ITO electrodes, a TFT was assembled using the structures of Type II as source- and drain-contacts. After the ITO contacts were formed, the active layer was deposited by spin-coating a ZnO nanoparticle dispersion onto the samples. A fully printed TFT based on nanoparticulate materials will be addressed in future work.

For the deposition of electrodes for the assembly of a TFT via the MIMIC technique, hydrophilic stamps of Type II were used. As the structures of Type II exhibit rectangular bendings, a hydrophilized stamp was used to assure complete infiltration of the stamp. For the construction of the TFT, a bottom gate assembly on an oxidized silicon wafer was desired (see Fig. 3). Therefore, structures of Type II were deposited on a thermally oxidized silicon wafer using the hydrophilic stamps and the ethanol-based dispersion with 20 wt% (2.70 vol.%) ITO. The contact angle between the dispersion and the wafer was 8.26°, i.e., the wetting of the dispersion on the substrate was good. A topographical picture of an exemplary structure is shown in Fig. 8. The roughness R_a of the structure is 15 nm, the height at the edges 0.75 μm, and the height depression is 41.33%. Thus, structures of Type II feature an increased roughness, a smaller height, and an increased height depression compared to structures of Type I (see Table 3).
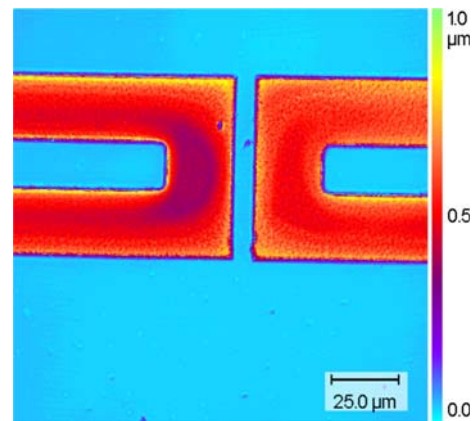

Fig. 8 Topographical picture of a structure of Type II printed with a hydrophilic stamp and the ethanol-based dispersion with 20 wt% (2.70 vol.%) ITO on oxidized wafer

This can be explained by the longer channels, which form the supplies, and the 90° change in direction of the Type II structure, which both hinder optimal particle transport.

The electrical characteristics of the TFT assembled with the structure of Type II are depicted in Figs. 9 and 10. A drain current modulation with varying gate voltage is observed and therefore the functionality of the deposited structures is demonstrated. Nevertheless, the TFT requires further optimization: obviously, a high gate leakage current exists because a negative drain current I_D is observed at a positive gate-source voltage V_{GS} at zero drain-source voltage V_{DS}. This indicates an insufficient quality of the dielectric layer, which could be due to contamination introduced by the nano-particulate dispersions. The charge carrier mobility of 6×10^{-3} cm^2/Vs and an I_{on}/I_{off}-ratio of more than 10^3 measured for our device is in the range of values calculated for TFTs based on the same ZnO nano-particulate dispersion with aluminum source/drain contacts deposited by thermal evaporation.
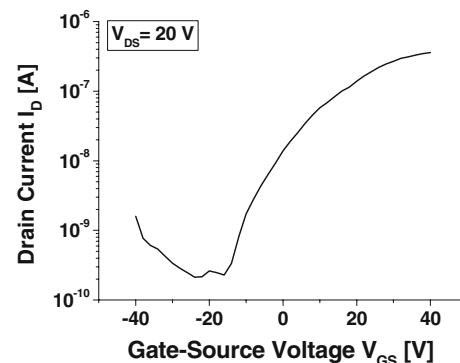

Fig. 9 Transfer characteristics of the TFT based on ZnO nano-particulate dispersion with ITO source/drain contacts printed by MIMIC
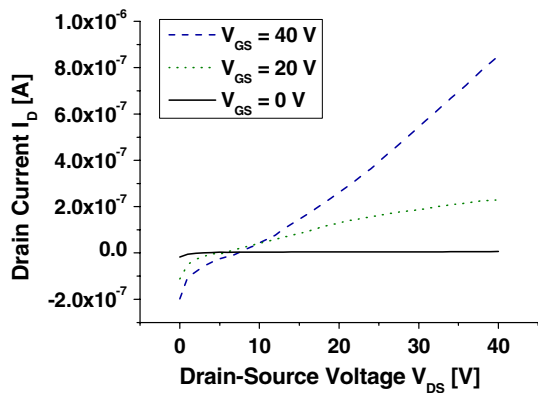
Fig. 10 Output characteristics of the TFT based on a ZnO nano-particulate dispersion with ITO source/drain contacts printed by MIMIC

Conclusions

In this work, the applicability of the soft lithographic technique MIMIC for the manufacture of electrically functional structures in the range of a few microns was successfully demonstrated.

Indium tin oxide nano-particles were sterically stabilized in ethanol as well as electrostatically stabilized in water. Both dispersions exhibited viscosities low enough to be suitable for the infiltration during the MIMIC process. The optimum particle content in the dispersions with regard to further processing via soft lithographic printing was determined by particle size measurements and first infiltration experiments to be ~ 20 wt%, i.e., 2.70 vol.% in sterically stabilized dispersions.

A significant influence of the wetting behavior of the used dispersions on the resulting geometry of the structures was detected. The high surface tension of the water leads to large contact angles between the water-based dispersions and the substrate and stamp materials used. This caused an island-like distribution of the particles in the channel. A low contact angle was measured between ethanol-based dispersions and the used glass substrates. This wetting behavior lead to a good reproduction of the stamp geometry. Furthermore, the geometry of the printed structures could be adapted by surface-functionalization of the stamp material. Thus, the wetting behavior of the dispersions on the stamp could be controlled. Structure heights of about 2 μm, structure widths of 25 μm, and roughness values R_a down to 3 nm could be realized.

Finally, the functionality of the structures could be successfully demonstrated by the assembly of a TFT. The device was built up on a thermally oxidized silicon wafer, which provided the bottom gate and the dielectric. The semiconducting layer was deposited by spin coating a ZnO nano-particulate dispersion onto the top electrodes, which were printed by soft lithographic methods.

In summary, the results obtained in this work demonstrate the high potential of particulate, nano-sized dispersions for the manufacture of printed electron devices. For flexible displays, flexible solar cells, etc., ITO dispersions are suitable to supply the desired transparent and conductive structures.

References

1. Dimitrakopoulos CD, Malenfant PRL (2002) Adv Mater 14:99
2. Loo Y-L, McCulloch I (2008) MRS Bull 33:653
3. Sekitani T, Noguchi Y, Zschieschang U, Klauk H, Someya T (2008) Proc Natl Acad Sci USA 105:4976
4. Kim S-M, Seo K-H, Lee J-H, Kim J-J, Lee HY, Lee J-S (2006) J Eur Ceram Soc 26:73
5. Delamarche E, Juncker D, Schmid H (2005) Adv Mater 17:2911
6. Jeon NL, Clem P, Jung DY, Lin W, Girolami GS, Payne DA, Nuzzo RG (1997) Adv Mater 9:891
7. Parashkov R, Becker E, Riedl T, Johannes H-H, Kowalsky W (2005) Adv Mater 17:1523
8. Cosseddu P, Bonfiglio A (2006) Appl Phys Lett 88:1
9. Blümel A, Klug A, Eder S, Scherf U, Moderegger E, List EJW (2007) Org Electron 8:389
10. Zschieschang U, Halik M, Klauk H (2008) Langmuir 24:1665
11. Xia Y, Whitesides GM (1998) Annu Rev Mater Sci 28:153
12. Ahn BY, Duoss EB, Motala MJ, Guo X, Park S-I, Xiong Y, Yoon J, Nuzzo RG, Rogers JA, Lewis JA (2009) Science 323:1590
13. Reindl A, Mahajeri J, Peukert W (2009) Thin Solid Films 517:1624
14. de Hazan Y, Heinecke J, Weber A, Graule T (2009) J Colloid Interf Sci 337:66
15. de Hazan Y, Reuter T, Werner D, Clasen R, Graule T (2008) J Colloid Interf Sci 323:293
16. Widegren J, Bergström L (2002) J Am Ceram Soc 85:523
17. Rogers JA, Nuzzo RG (2005) Mater Today 8:50
18. Schmitt H, Zeidler M, Rommel M, Bauer AJ, Ryssel H (2008) Microelectron Eng 85:897
19. Delamarche E, Donzel C, Kamounah FS, Wolf H, Geissler M, Stutz R, Schmidt-Winkel P, Michel B, Mathieu HJ, Schaumburg K (2003) Langmuir 19:8749
20. Gross M, Winnacker A, Wellmann PJ (2007) Thin Solid Films 515:8567
21. Lutz C, Roosen A (1998) Wetting behaviour of tape casting slurries on tape carriers. In: Messing GL, Lange FF, Hirano S (eds) Ceramic transactions, vol 83. The American Ceramic Society, Columbus, OH, pp 163–170
22. Martin CR, Aksay IA (2003) J Phys Chem B 107:4261
23. Delamarche E, Schmid H, Biebuyck H, Michel B (1997) Adv Mater 9:741
24. Hsia KJ, Huang Y, Menard E, Park J-U, Zhou W, Rogers J, Fulton JM (2005) Appl Phys Lett 86:1
25. Huang YY, Zhou W, Hsia KJ, Menard E, Park J-U, Rogers JA, Alleyne AG (2005) Langmuir 21:8058
26. Granqvist CG, Hultåker A (2002) Thin Solid Films 411:1